Acta Cryst E CRYSTALLOGRAPHIC COMMUNICATIONS
ISSN 2056-9890

Distinct coordination geometries in bis[*N*,*N*-bis(2-methoxyethyl)dithiocarbamato-κ^2S,S']diphenyltin(IV) and bis[*N*-(2-methoxyethyl)-*N*-methyldithiocarbamato-κ^2S,S']diphenyltin(IV): crystal structures and Hirshfeld surface analysis

Received 11 July 2016
Accepted 13 July 2016

Edited by W. T. A. Harrison, University of Aberdeen, Scotland

‡ Additional correspondence author, e-mail: awang_normah@yahoo.com.

Keywords: crystal structure; organotin; dithiocarbamate; Hirshfeld surface analysis.

CCDC references: 1492701; 1492700

Supporting information: this article has supporting information at journals.iucr.org/e

Rapidah Mohamad,[a] Normah Awang,[b]‡ Mukesh M. Jotani[c] and Edward R. T. Tiekink[d]*

[a]Biomedical Science Programme, School of Diagnostic and Applied Health Sciences, Faculty of Health Sciences, Universiti Kebangsaan Malaysia, Jalan Raja Muda Abdul Aziz, 50300 Kuala Lumpur, Malaysia, [b]Environmental Health and Industrial Safety Programme, School of Diagnostic and Applied Health Sciences, Faculty of Health Sciences, Universiti Kebangsaan Malaysia, Jalan Raja Muda Abdul Aziz, 50300 Kuala Lumpur, Malaysia, [c]Department of Physics, Bhavan's Sheth R. A. College of Science, Ahmedabad, Gujarat 380 001, India, and [d]Research Centre for Chemical Crystallography, Faculty of Science and Technology, Sunway University, 47500 Bandar Sunway, Selangor Darul Ehsan, Malaysia. *Correspondence e-mail: edwardt@sunway.edu.my

The crystal and molecular structures of two diphenyltin bis(dithiocarbamate)s, $[Sn(C_6H_5)_2(C_5H_{10}NOS_2)_2]$, (I), and $[Sn(C_6H_5)_2(C_7H_{14}NO_2S_2)_2]$, (II), are described. In (I), in which the metal atom lies on a twofold rotation axis, the dithiocarbamate ligand coordinates with approximately equal Sn—S bond lengths and the *ipso*-C atoms of the Sn-bound phenyl groups occupy *cis*-positions in the resulting octahedral C_2S_4 donor set. A quite distinct coordination geometry is noted in (II), arising as a result of quite disparate Sn—S bond lengths. Here, the four S-donors define a trapezoidal plane with the *ipso*-C atoms lying over the weaker of the Sn—S bonds so that the C_2S_4 donor set defines a skewed trapezoidal bipyramid. The packing of (I) features supramolecular layers in the *ab* plane sustained by methylene-C—H$\cdots\pi$(Sn–aryl) interactions; these stack along the *c*-axis direction with no specific interactions between them. In (II), supramolecular chains along the *b*-axis direction are formed by methylene-C—O(ether) interactions; these pack with no directional interactions between them. A Hirshfeld surface analysis was conducted on both (I) and (II) and revealed the dominance of H$\cdots$H interactions contributing to the respective surfaces, *i.e.* >60% in each case, and other features consistent with the description of the molecular packing above.

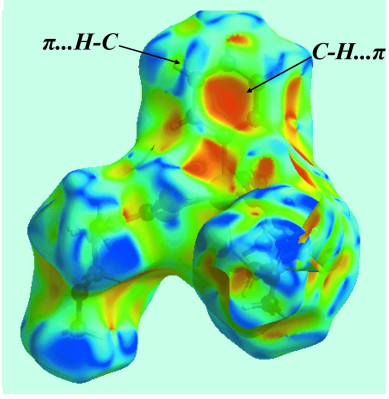

OPEN ACCESS

1. Chemical context

In a review of the applications and structures of tin/organotin dithiocarbamates (dithiocarbamate is $^-S_2CNRR'$; *R*, *R*′ = alkyl, aryl), two applications were highlighted, namely, their potential biological activity and their utility as single-source precursors for tin sulfide nanoparticles (Tiekink, 2008). Investigations in both fields continue, *e.g.* as anti-cancer agents (Khan *et al.*, 2014, 2015; Kadu *et al.*, 2015), as anti-microbials (Zia-ur-Rehman *et al.*, 2011; Ferreira *et al.*, 2012, 2014) and as fungicides (Yu *et al.*, 2014). The use of various tin dithiocarbamate species as precursors for tin sulfide materials also continues to attract significant attention (Ramasamy *et al.*, 2013; Lewis *et al.*, 2014; Kevin *et al.*, 2015). It was during the course of ongoing studies of the anti-tumour potential of

organotin dithiocarbamates (Khan *et al.*, 2014, 2015) that attention was directed towards (2-methoxyethyl)dithiocarbamate derivatives. Herein, the crystal and molecular structures of two diphenyltin derivatives, *viz*. $[Sn(C_6H_5)_2(C_5H_{10}NOS_2)_2]$, (I), and $[Sn(C_6H_5)_2(C_7H_{14}NOS_2)_2]$, (II), are reported that exhibit quite distinct coordination geometries, along with a Hirshfeld surface analysis to provide more details on the molecular packing.

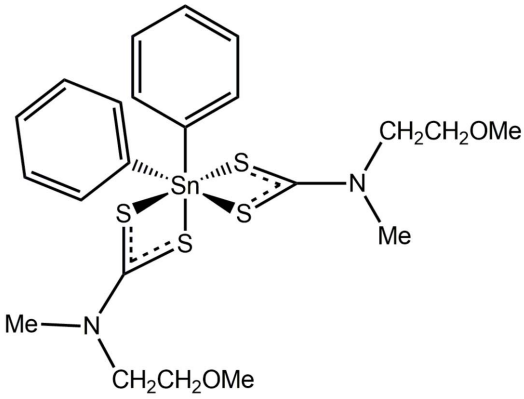

(I)

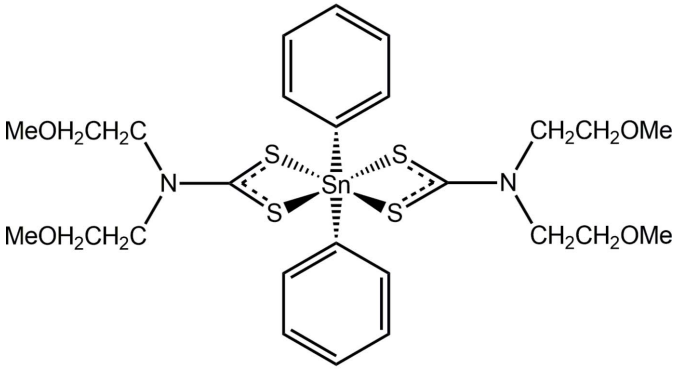

(II)

1.1. Structural commentary

The asymmetric unit of (I) comprises half a molecule as the tin atom is located on a twofold rotation axis, Fig. 1. The C_2S_4 donor set is defined by two chelating dithiocarbamate ligands and the *ipso*-carbon atoms of the tin-bound phenyl substituents. The difference between the $Sn-S_{short}$ and $Sn-S_{long}$ bond lengths, *i.e.* Δ(Sn—S), is relatively small at 0.06 Å, indicating an essentially symmetric coordination mode. This symmetry is reflected in the near equivalence of the associated C1—S bond lengths with the difference between them being 0.024 Å, Table 1. The longer Sn—S2 bond is approximately *trans* to the *ipso*-carbon atom. The overall coordination geometry is based on an octahedron with the *ipso*-carbon atoms occupying mutually *cis* positions. The methoxyethyl group is approximately perpendicular to the S_2CN core as seen in the value of the C1—N1—C3—C4 torsion angle of 93.8 (2)°. The residue itself is almost planar and adopts an extended conformation as seen in the C5—O1—C4—C3 torsion angle of 175.27 (19)°.

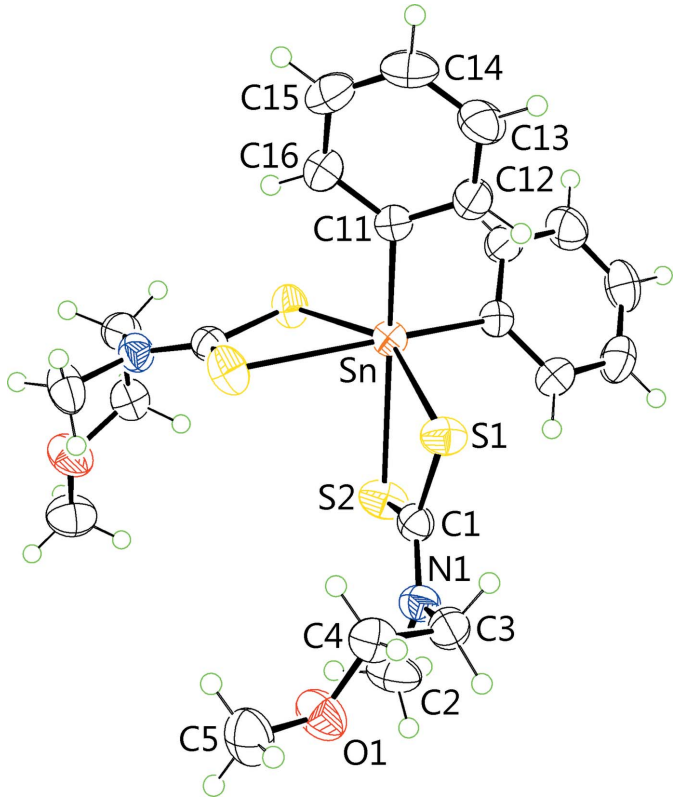

Figure 1
The molecular structure of (I), showing the atom-labelling scheme and displacement ellipsoids at the 50% probability level. Unlabelled atoms are related by the symmetry operation $(1-x, y, \frac{3}{2}-z)$.

The molecule in (II), Fig. 2, lies on a general position and has a quite distinct coordination geometry. As for (I), the tin atom is located within a C_2S_4 donor set. However, the dithiocarbamate ligand is coordinating with significantly greater values of ΔS, *i.e.* 0.48 and 0.46 Å for the S1- and S3-ligands,

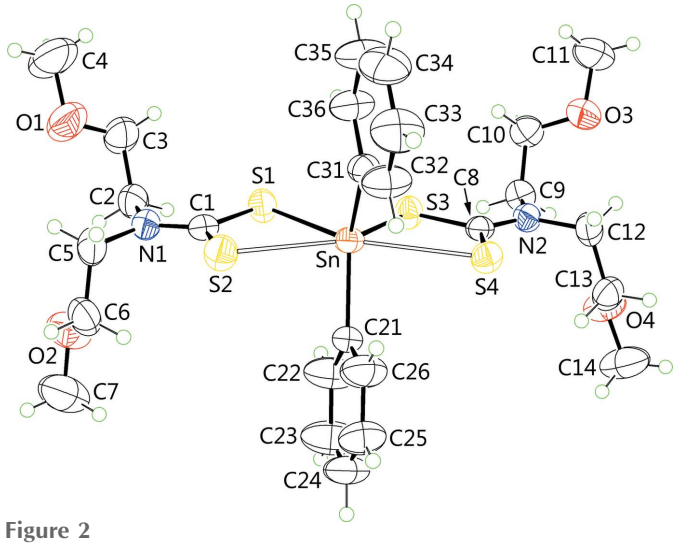

Figure 2
The molecular structure of (II), showing the atom-labelling scheme and displacement ellipsoids at the 50% probability level.

Table 1
Geometric data (Å, °) for (I) and (II).

Parameter	(I)	(II)
Sn—S1	2.6071 (6)	2.5060 (6)
Sn—S2	2.6653 (6)	2.9875 (6)
Sn—S3	–	2.5230 (6)
Sn—S4	–	2.9800 (6)
Sn—C11	2.1677 (18)	–
Sn—C21	–	2.131 (2)
Sn—C31	–	2.124 (2)
C1—S1	1.7311 (19)	1.756 (2)
C1—S2	1.7067 (19)	1.692 (2)
C8—S3	–	1.752 (2)
C8—S4	–	1.692 (2)
S1^{i}—Sn—S2^{i}	67.742 (17)	64.922 (18)
S3—Sn—S4	–	64.591 (16)
S1—Sn—S1^{i}	152.00 (2)	–
S2^{i}—Sn—C11^{i}	159.03 (5)	–
S1—Sn—S3	–	82.873 (18)
S2—Sn—S4	–	147.642 (17)
C—Sn—C	100.07 (10)	130.12 (9)

Symmetry code: (i) $1-x, y, \frac{3}{2}-z$.

respectively, with the Sn—S_{short} bonds in (II) being shorter than the equivalent bonds in (I) and at the same time, the Sn—S_{long} bonds in (II) being longer than those in (I). An interesting consequence of the different modes of coordination of the dithiocarbamate ligands in the two structures is that the Sn—C_{bond} lengths in (II) are considerably shorter than those in (I), Table 1. As the dithiocarbamate anions are approximately co-planar and the more tightly bound S1 and S3 atoms lie to the same side of the molecule, the S_4 donor atoms define a trapezoidal plane. The tin-bound *ipso*-carbon atoms are disposed over the weaker Sn—S bonds so that the coordination geometry is skewed trapezoidal bipyramidal. Reflecting the significant disparity in the Sn—S bonds, there are large differences in the associated C—S bonds with the shorter of these being associated with the weakly coordinating sulfur atoms, Table 1. As for (I), the methoxyethyl groups lie almost perpendicular to the plane through the S_2CN atoms with the greatest deviation being for the O1-containing residue, *i.e.* the C1—N1—C5—C6 torsion angle is −81.5 (3)°. For each dithiocarbamate ligand, the residues lie to either side of the S_2CN plane, and each is as for (I), adopting an almost planar and extended conformation with the O4-residue showing the greatest deviation, albeit marginally, as seen in the C14—O4—C13—C12 torsion angle of 176.3 (2)°.

Table 2
Hydrogen-bond geometry (Å, °) for (I).

*Cg*1 is the centroid of the C11–C16 phenyl ring.

D—H···*A*	*D*—H	H···*A*	*D*···*A*	*D*—H···*A*
C4—H4*A*···*Cg*1^{i}	0.97	2.86	3.730 (3)	150

Symmetry code: (i) $x+1, -y, z+\frac{1}{2}$.

Table 3
Hydrogen-bond geometry (Å, °) for (II).

D—H···*A*	*D*—H	H···*A*	*D*···*A*	*D*—H···*A*
C13—H13*A*···O2^{i}	0.97	2.52	3.404 (4)	151

Symmetry code: (i) $x, y-1, z$.

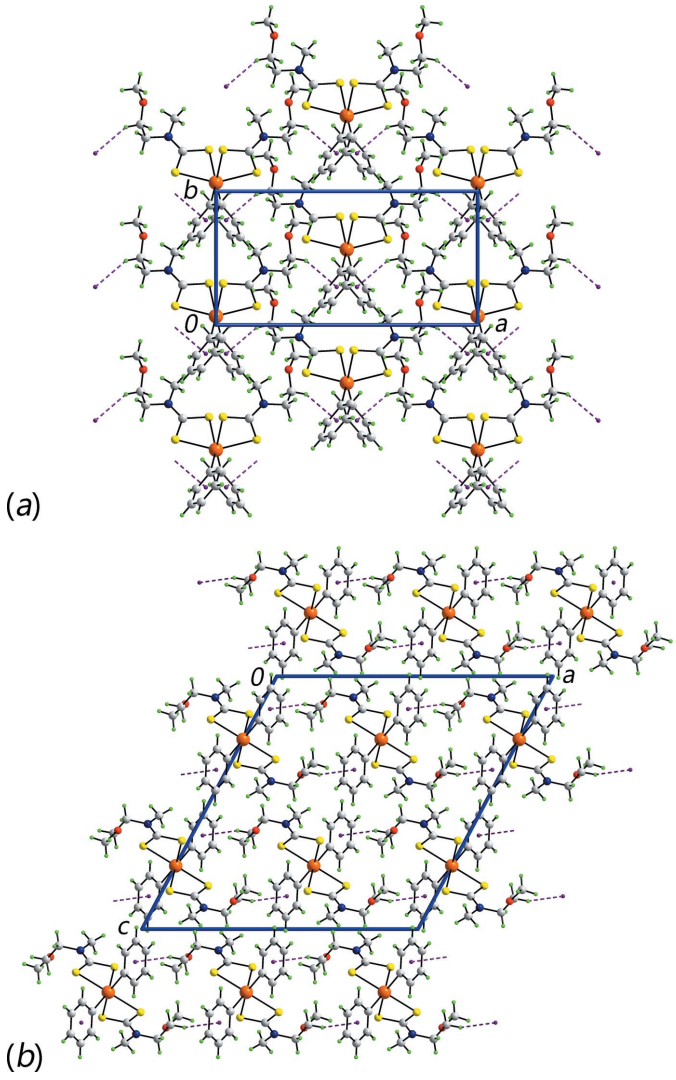

Figure 3
Molecular packing in (I), showing (*a*) a supramolecular layer in the *ab* plane sustained by methylene-C—H···π(Sn-phenyl) interactions (purple dashed lines) and (*b*) a view of the unit-cell contents in projection down the *b* axis.

2. Supramolecular features

Geometric parameters characterizing the intermolecular interactions operating in the crystal structures of (I) and (II) are collected in Tables 2 and 3, respectively. Based on the distance criteria in *PLATON* (Spek, 2009), the only significant intermolecular contact in the molecular packing of (I) is a methylene-C—H···π(Sn–aryl) interaction. From symmetry, there are four such interactions per molecule so that a two-dimensional supramolecular layer in the *ab* plane ensues, Fig. 3*a*. These stack along the *c* axis being separated by hydrophobic interactions, Fig. 3*b*.

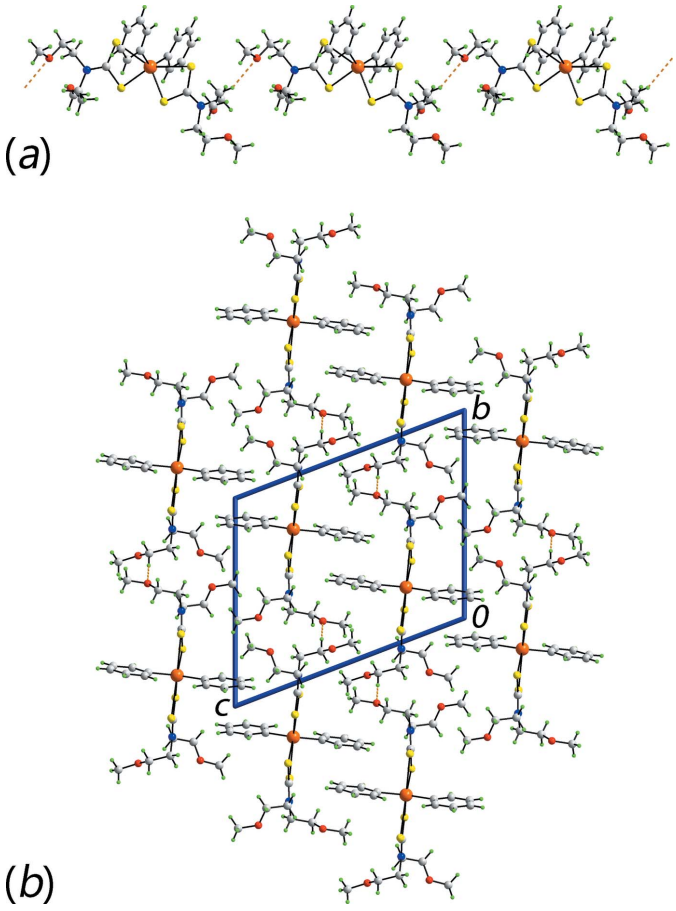

Figure 4
Molecular packing in (II), showing (*a*) a supramolecular chain along the *b* axis sustained by methylene-C—H···O interactions (orange dashed lines) and (*b*) a view of the unit-cell contents in projection down the *a* axis.

In the molecular packing of (II), methylene-C—H···O interactions lead to linear supramolecular chains along the *b* axis, Fig. 4*a*. These pack into the three-dimensional architecture of the crystal with no directional intermolecular interactions between them, Fig. 4*b*.

A more detailed analysis of the molecular packing in (I) and (II) is given below in Hirshfeld surface analysis.

3. Hirshfeld surface analysis

Hirshfeld surfaces for (I) and (II) were mapped over d_{norm}, d_e, shape-index, curvedness and electrostatic potential with the aid of *Crystal Explorer 3.1* (Wolff *et al.*, 2012). The electrostatic potentials were calculated using *TONTO* (Spackman *et al.*, 2008; Jayatilaka *et al.*, 2005), integrated into *Crystal Explorer*, and were mapped on the Hirshfeld surfaces using the STO-3G basis set at Hartree–Fock level of theory over the range ±0.12 au. The contact distances d_e and d_i from the Hirshfeld surface to the nearest atom inside and outside, respectively, enables the analysis of the intermolecular interactions through the mapping of d_{norm}. The combination of d_e and d_i in the form of

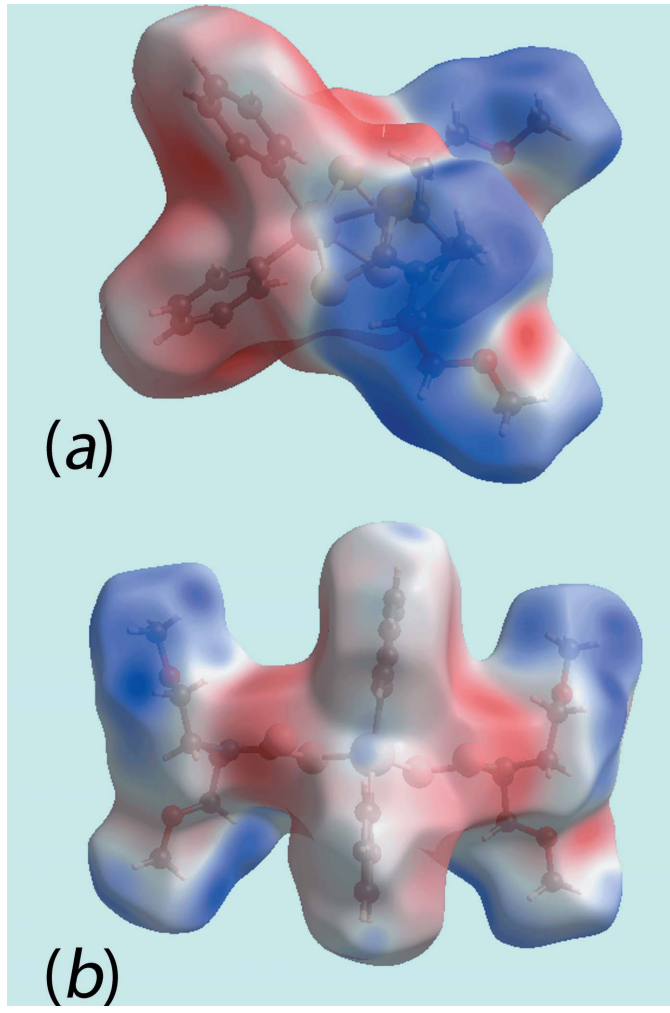

Figure 5
View of Hirshfeld surfaces mapped over the electrostatic potential (the red and blue regions represent negative and positive electrostatic potentials, respectively): (*a*) for (I) and (*b*) for (II).

two-dimensional fingerprint plots (McKinnon *et al.*, 2007) provides a visual summary of intermolecular contacts in the crystal.

As evident from Fig. 5, the Hirshfeld surfaces for (I) and (II) have quite different shapes reflecting the distinctive coordination geometries, and the dark-red and dark-blue regions assigned to negative and positive potentials are localized near the respective functional groups. The absence of conventional hydrogen bonds in the crystal of (I) is consistent with the non-appearance of characteristic red spots in the calculated Hirshfeld surface mapped over d_{norm} (not shown). By contrast, in (II), the weak C—H···O interaction gives rise to red spots as evident in Fig. 6.

The overall two-dimensional fingerprint plots for (I) and (II) and those delineated into H···H, O···H/H···O, C···H/H···C and S···H/H···S contacts are illustrated in Fig. 7; their relative contributions are summarized in Table 4. The different distribution of points in the overall fingerprint plots for (I) and (II) are due to their different molecular conformations. Also, it is noted that the points are distributed in

Table 4
Percentage contribution of the different intermolecular contacts to the Hirshfeld surface in (I) and (II).

Contact	% contribution in (I)	% contribution in (II)
H···H	61.8	66.1
C···H/H···C	15.6	11.4
O···H/H···O	4.7	7.4
S···H/H···S	15.6	13.5
C···S/S···C	1.3	0.0
N···H/H···N	1.0	0.4
C···C	0.0	1.0
S···S	0.0	0.1
C···O/O···C	0.0	0.1

different (d_e, d_i) ranges, *i.e.* 1.2 to 2.7 Å for (I) and 1.2 to 2.9 Å for (II).

As evident from the data in Table 4 and the fingerprint plots in Fig. 7*b*, H···H contacts clearly make the most significant contributions to the Hirshfeld surfaces of both (I) and (II). In the fingerprint plot of (I) delineated into H···H contacts

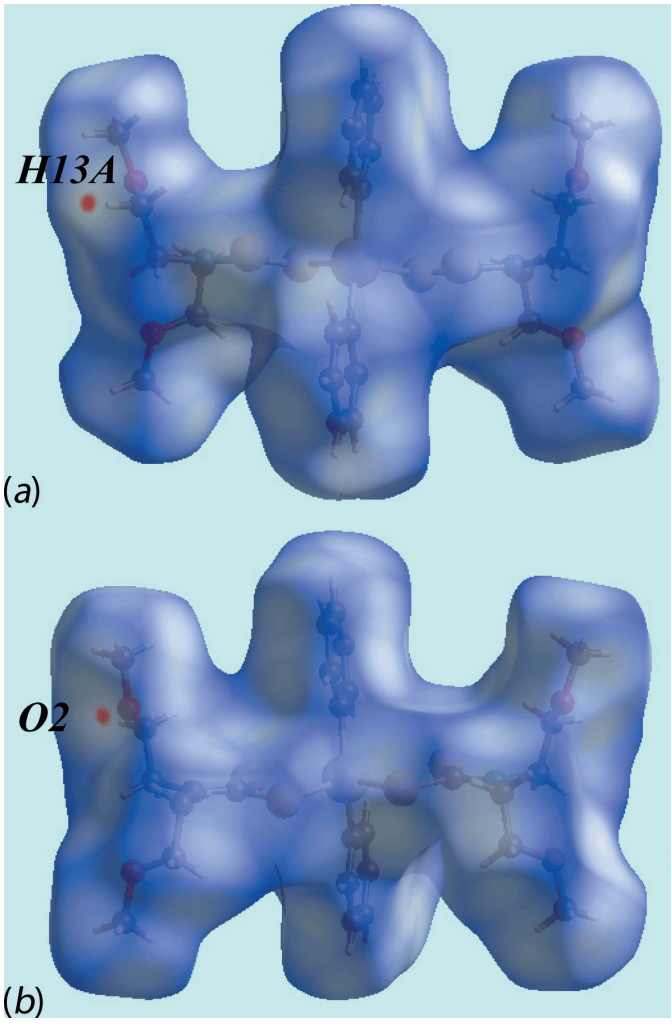

Figure 6
Views of Hirshfeld surfaces mapped over d_{norm} for (II).

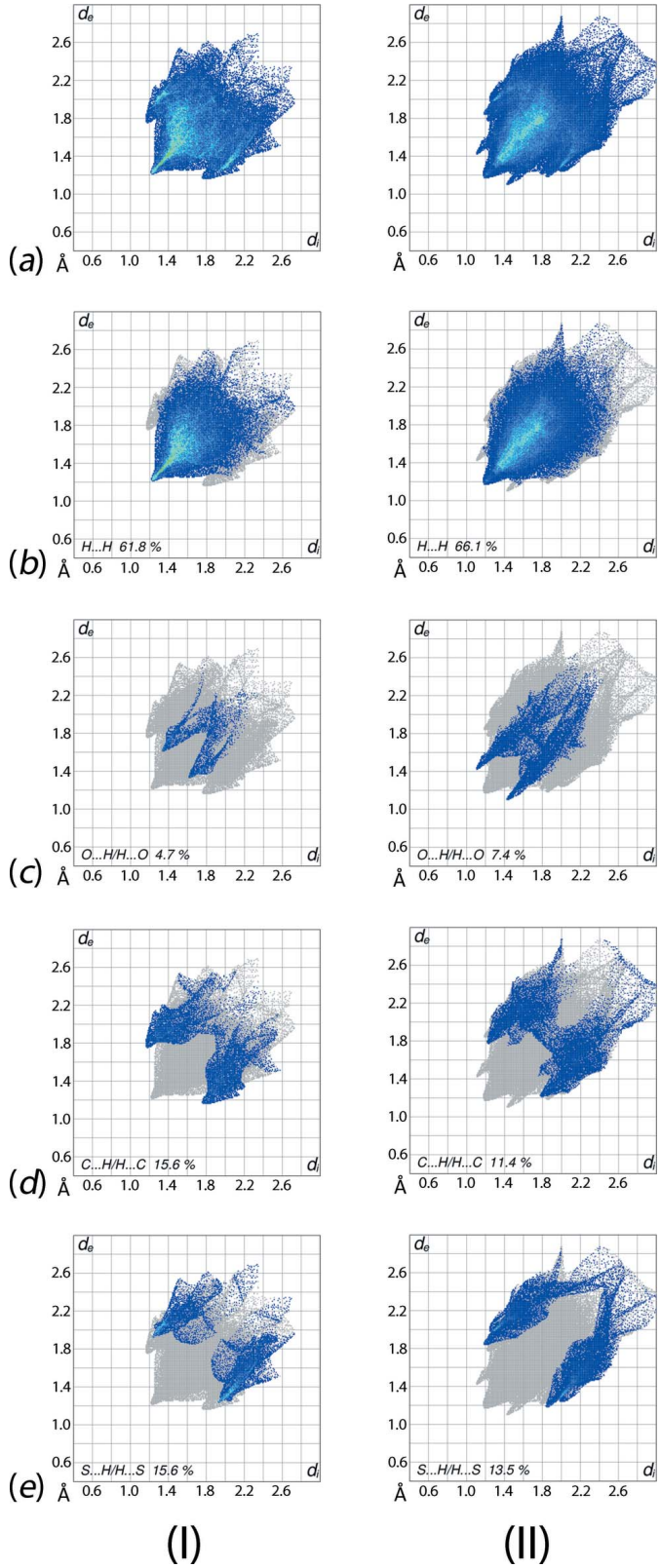

Figure 7
Comparison of the (*a*) complete Hirshfeld surface and full two-dimensional fingerprint plots between (I) and (II), and the plots delineated into (*b*) H···H, (*c*) O···H/H···O, (*d*) C···H/H···C and (*e*) S···H/H···S contacts.

Table 5
Short interatomic contacts in (II).

Contact	distance	symmetry operation
O4···H6*B*	2.69	−1 − *x*, *y*, *z*
H7*C*···H14*B*	2.37	1 + *x*, *y*, *z*
H10*B*···H34	2.36	1 − *x*, −*y*, −*z*

(Fig. 7*b*), all the points are situated at (d_e, d_i) distances equal to or greater than their van der Waals separations *i.e.* 1.2 Å, reflecting zero propensity to form such intermolecular contacts. By contrast, for (II), points at (d_e, d_i) distances less than 1.2 Å, with the peak at $d_e = d_i$ ~1.2 Å, resulting from short interatomic H···H contacts, Table 5. The 7.4% contribution from O···H/H···O contacts to the Hirshfeld surface of (II) reflects the presence of an intermolecular C—H···O interaction and a short interatomic O···H/H···O contact (Table 5), showing a forceps-like distribution of points with the tips at $d_e + d_i$ ~2.5 Å in Fig. 7*c*. The small contribution, *i.e.* 4.7%, due to analogous interactions in (I) have a low density of points that are generally masked by other contacts in the plot consistent with a low propensity to form.

The pair of characteristics wings with the edges at $d_e + d_i$ ~2.9 Å in the fingerprint plot delineated into C···H/H···C contacts for (I) is due to the contribution of methylene-C—H···π(Sn–aryl) interactions, Fig. 7*d*. The presence of these interactions are also indicated through the pale-orange spots present on the Hirshfeld surface mapped over d_e, shown within the blue circle in Fig. 8*a*, and bright-red spots over the front side of shape-indexed surfaces identified with arrows in Fig. 8*b*. The reciprocal of these C—H···π contacts, *i.e.* π···H—C contacts, are seen as blue spots near the ring in Fig. 8*b*. The fingerprint plot for (II) delineated into C···H/H···C contacts has a distinct distribution of points with the (d_e, d_i) distances greater than their van der Waals separations, confirming the absence of these interactions, Fig. 7*d*. The conformations of dithiocarbamate ligands in both (I) and (II) limit the sulfur atoms' ability to form significant S···H intermolecular interactions; these atoms are separated at distances greater than their van der Waals radii, *i.e.* 3.0 Å. This observation is despite the nearly symmetrical distributions of points in the respective plots for both (I) and (II), Fig. 7*e*, and the significant percentage contributions to their Hirshfeld surfaces (Table 5).

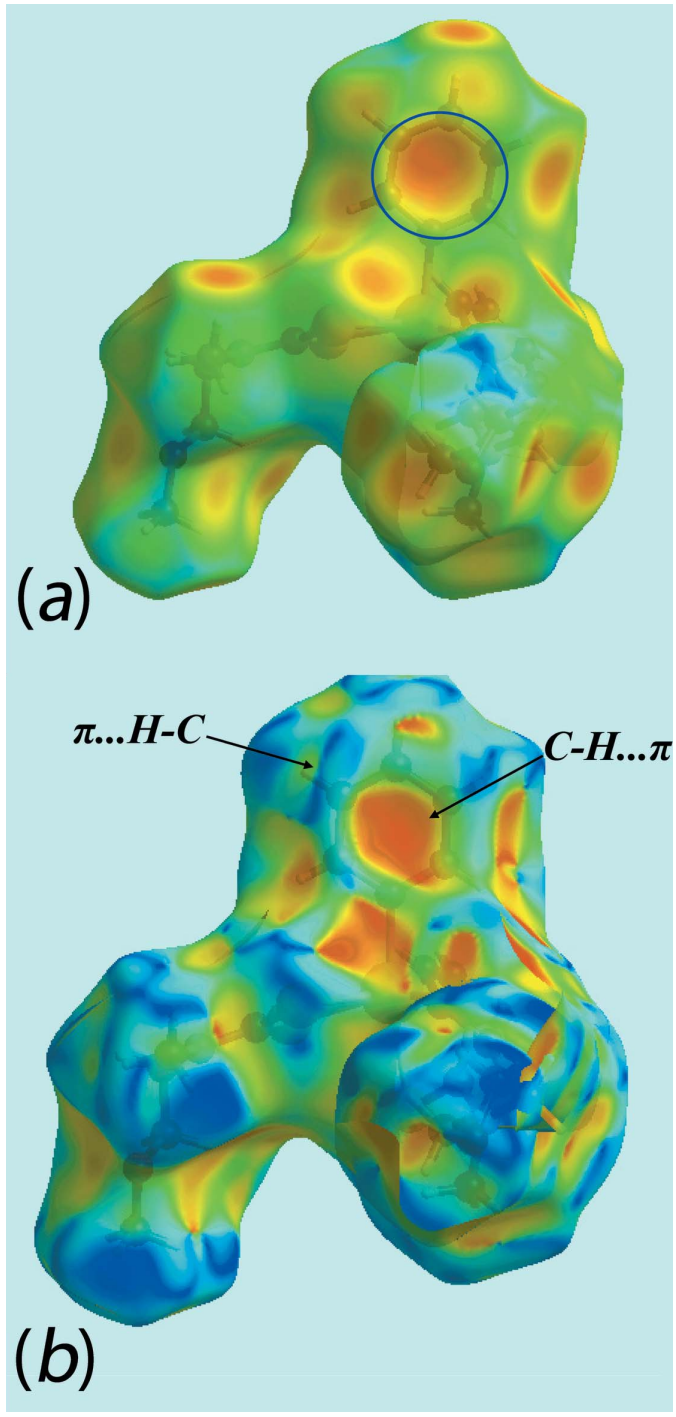

Figure 8
View of the Hirshfeld surfaces for (I), showing (*a*) mapped over d_e with the pale-orange spot within the blue circle indicating the involvement of the aryl ring in C—H···π interactions and (*b*) mapped with the shape-index property with the bright-red spot, identified with an arrow, indicating the C—H···π interaction and the blue spots indicating complementary π···H—C interactions.

4. Database survey

Given the various applications found for tin dithiocarbamates, it is not surprising that there exists a relatively large number of structures for this class of compound. Indeed, a search of the Cambridge Structural Database (CSD; Groom *et al.*, 2016), reveals over 300 'hits'. Structural surveys have revealed that very different coordination geometries can arise in the solid state and, even when a common structural motif is adopted, non-systematic variations in geometric parameters are observed (Tiekink, 2008; Muthalib *et al.*, 2014). Mononuclear diorganotin bis(dithiocarbamate)s, *i.e.* directly related to (I) and (II) described herein, are well represented, there being about 90 examples. Four distinct structural motifs have been noted previously (Tiekink, 2008), and these are illustrated in

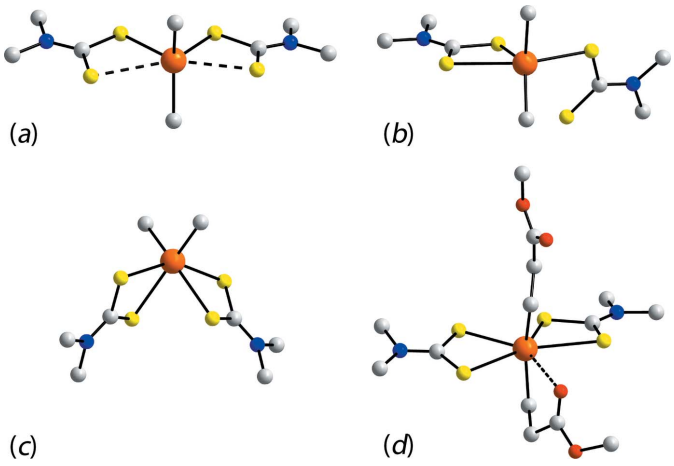

Figure 9
Four structural motifs for molecules of the general composition $R_2Sn(S_2CNR'R'')_2$: (*a*) skew trapezoidal bipyramidal, (*b*) five-coordinate trigonal–bipyramidal owing to a monodentate dithiocarbamate ligand, (*c*) *cis*-octahedral and (*d*) seven-coordinate pentagonal–bipyramidal owing to additional coordination by a heteroatom of the tin-bound residue. In all images, H atoms have been omitted, only the α-C atoms bound to nitrogen included and, in all but (*d*), only the α-C atom of the tin-bound residues shown.

Fig. 9. The two most common motifs are skewed trapezoidal bipyramidal as in (II), Fig. 9*a*, and distorted octahedral, as in (I), Fig. 9*c*. Less common are five-coordinate, trigonal–bipyramidal species, arising as one dithiocarbamate ligand is monodentate, Fig. 9*b*, are found, for example, in the structure of $(t\text{-Bu})_2Sn(S_2CNMe_2)_2$ (Kim *et al.*, 1987) and correlated with bulky tin-bound groups, and seven-coordinate species, pentagonal–bipyramidal, owing to additional coordination by a heteroatom of the tin-bound residue, Fig. 9*d*, as for example in the structure of $[MeOC(=O)CH_2CH_2]_2Sn(S_2CNMe)_2$ (Ng *et al.*, 1989).

There are 16 diphenyltin bis(dithiocarbamate) structures included in the CSD and eight of these adopt the motif shown in Fig. 9*c*, including both the monoclinic (Lindley & Carr, 1974) and twofold symmetric tetragonal (Hook *et al.*, 1994) polymorphs of the archetype compound $Ph_2Sn(S_2CNEt_2)_2$, and eight adopt the motif shown in Fig. 9*a*, including both independent molecules of $Ph_2Sn[S_2CN(Me)Hex]_2$ (Ramasamy *et al.*, 2013); the remaining structures are single phase and have one independent molecule. Such an even split suggests a fine energy balance between the adoption of one geometry over the other.

5. Synthesis and crystallization

Synthesis of (I). (2-Methoxyethyl)methylamine (2 mmol) dissolved in ethanol (10 ml) was stirred in an ice-bath for 30 min. A 25% ammonia solution (1–2 ml) was added to generate a basic solution. Then, a cold ethanolic solution of carbon disulfide (2 mmol) was added to the solution and stirred for about 2 h. Next, diphenyltin(IV) dichloride

Table 6
Experimental details.

	(I)	(II)
Crystal data		
Chemical formula	$[Sn(C_6H_5)_2(C_5H_{10}NOS_2)_2]$	$[Sn(C_6H_5)_2(C_7H_{14}NO_2S_2)_2]$
M_r	601.41	689.51
Crystal system, space group	Monoclinic, *C*2/*c*	Triclinic, $P\overline{1}$
Temperature (K)	293	293
a, *b*, *c* (Å)	18.3808 (14), 8.2809 (4), 19.083 (3)	7.4386 (4), 14.3334 (8), 16.5398 (10)
α, β, γ (°)	90, 118.071 (8), 90	110.320 (5), 91.282 (5), 101.865 (4)
V (Å^3)	2562.9 (5)	1609.93 (17)
Z	4	2
Radiation type	Mo *K*α	Mo *K*α
μ (mm^{-1})	1.34	1.09
Crystal size (mm)	0.25 × 0.25 × 0.20	0.30 × 0.25 × 0.25
Data collection		
Diffractometer	Agilent Technologies SuperNova Dual diffractometer with Atlas detector	Agilent Technologies SuperNova Dual diffractometer with Atlas detector
Absorption correction	Multi-scan (*CrysAlis PRO*; Agilent, 2015)	Multi-scan (*CrysAlis PRO*; Agilent, 2015)
T_{min}, T_{max}	0.815, 1.000	0.756, 1.000
No. of measured, independent and observed [$I > 2\sigma(I)$] reflections	7357, 3383, 3051	17063, 8354, 6973
R_{int}	0.025	0.035
(sin $\theta/\lambda)_{max}$ (Å^{-1})	0.712	0.712
Refinement		
$R[F^2 > 2\sigma(F^2)]$, $wR(F^2)$, *S*	0.026, 0.063, 1.07	0.031, 0.078, 1.06
No. of reflections	3383	8354
No. of parameters	143	338
H-atom treatment	H-atom parameters constrained	H-atom parameters constrained
$\Delta\rho_{max}$, $\Delta\rho_{min}$ (e Å^{-3})	0.47, −0.30	0.66, −0.56

Computer programs: *CrysAlis PRO* (Agilent, 2015), *SHELXL97* (Sheldrick, 2008), *SHELXL2014* (Sheldrick, 2015), *ORTEP-3 for Windows* (Farrugia, 2012), *DIAMOND* (Brandenburg, 2006) and *publCIF* (Westrip, 2010).

(1 mmol) dissolved in ethanol was added into the solution and further stirred for 2 h. The precipitate that formed was filtered off and washed a few times with cold ethanol to remove impurities. Finally, the precipitate was dried in a desiccator. Recrystallization was by dissolving the compound with chloroform and ethanol (2:1 *v*/*v*) ratio. This mixture was allowed to slowly evaporate at room temperature yielding colourless crystals of (I). m.p. 382–384 K. Yield: 78%. IR (cm^{-1}): 1,497 ν(C—N), 988 ν(C—S), 523 ν(Sn—C), 389 ν(Sn—S). ^{1}H NMR ($CDCl_3$): δ 7.28–8.00 (5H, Sn–Ph), 3.97 (2H, OCH_2), 3.69 (2H, NCH_2), 3.44 (3H, NMe), 3.36 (3H, OCH_3). ^{13}C NMR ($CDCl_3$): δ 199.88 (S_2C), 128.24–151.24 (Sn–Ar), 69.96 (OCH_2), 59.06 (NCH_2), 57.84 (OCH_3), 45.45 (NCH_3).

Compound (II) was prepared and recrystallized in essentially the same manner but using bis(2-methoxyethyl)amine (10 mmol) in place of (2-methoxyethyl)methylamine. m.p. 333–335 K. Yield: 76%. IR (cm^{-1}): 1,482 ν(C—N), 985 ν(C—S), 571 ν(Sn—C), 381 ν(Sn—S). ^{1}H NMR ($CDCl_3$): 7.38–7.89 (5H, Sn–Ph), 4.07 (2H, OCH_2), 3.77 (2H, NCH_2), 3.35 (OCH_3). ^{13}C NMR ($CDCl_3$): δ 200.16 (S_2C), 128.26–150.89 (Sn–Ar), 69.90 (OCH_2), 59.02 (NCH_2), 56.72 (OCH_3).

6. Refinement

Crystal data, data collection and structure refinement details are summarized in Table 6. Carbon-bound H-atoms were placed in calculated positions (C—H = 0.93–0.97 Å) and were included in the refinement in the riding model approximation, with U_{iso}(H) set to 1.2–1.5U_{eq}(C).

Acknowledgements

This work was supported by grant FRGS/2/2013/SKK10/UKM/02/1. We gratefully acknowledge the School of Chemical Science and Food Technology, Universiti Kebangsaan Malaysia for providing the essential laboratory facilities. We would also like to thank the laboratory assistants of the Faculty Science and Technology, Universiti Kebangsaan Malaysia for technical support. Intensity data were collected in the University of Malaya Crystallographic Laboratory.

References

Agilent (2015). *CrysAlis PRO*. Agilent Technologies Inc., Santa Clara, CA, USA.
Brandenburg, K. (2006). *DIAMOND*. Crystal Impact GbR, Bonn, Germany.
Farrugia, L. J. (2012). *J. Appl. Cryst.* **45**, 849–854.
Ferreira, I. P., de Lima, G. M., Paniago, E. B., Rocha, W. R., Takahashi, J. A., Pinheiro, C. B. & Ardisson, J. D. (2012). *Eur. J. Med. Chem.* **58**, 493–503.
Ferreira, I. P., de Lima, G. M., Paniago, E. B., Rocha, W. R., Takahashi, J. A., Pinheiro, C. B. & Ardisson, J. D. (2014). *Polyhedron*, **79**, 161–169.
Groom, C. R., Bruno, I. J., Lightfoot, M. P. & Ward, S. C. (2016). *Acta Cryst.* B**72**, 171–179.
Hook, J. M., Linahan, B. M., Taylor, R. L., Tiekink, E. R. T., van Gorkom, L. & Webster, L. K. (1994). *Main Group Met. Chem*. **17**, 293–311.
Jayatilaka, D., Grimwood, D. J., Lee, A., Lemay, A., Russel, A. J., Taylo, C., Wolff, S. K., Chenai, C. & Whitton, A. (2005). *TONTO – A System for Computational Chemistry*. Available at: http://hirshfeldsurface.net/
Kadu, R., Roy, H. & Singh, V. K. (2015). *Appl. Organomet. Chem.* **29**, 746–755.
Kevin, P., Lewis, D. J., Raftery, J., Malik, M. A. & O'Brien, P. (2015). *J. Cryst. Growth*, **415**, 93–99.
Khan, N., Farina, Y., Lo, K. M., Rajab, N. F. & Awang, N. (2014). *J. Mol. Struct.* **1076**, 403–410.
Khan, N., Farina, Y., Lo, K. M., Rajab, N. F. & Awang, N. (2015). *Polyhedron*, **85**, 754–760.
Kim, K., Ibers, J. A., Jung, O.-S. & Sohn, Y. S. (1987). *Acta Cryst.* C**43**, 2317–2319.
Lewis, D. J., Kevin, P., Bakr, O., Muryn, C. A., Malik, M. A. & O'Brien, P. (2014). *Inorg. Chem. Front.* **1**, 577–598.
Lindley, P. F. & Carr, P. (1974). *J. Cryst. Mol. Struct.* **4**, 173–185.
McKinnon, J. J., Jayatilaka, D. & Spackman, M. A. (2007). *Chem. Commun.* pp. 3814–3816.
Muthalib, A. F. A., Baba, I., Khaledi, H., Ali, H. M. & Tiekink, E. R. T. (2014). *Z. Kristallogr*. **229**, 39–46.
Ng, S. W., Wei, C., Kumar Das, V. G., Jameson, G. B. & Butcher, R. J. (1989). *J. Organomet. Chem.* **365**, 75–82.
Ramasamy, K., Kuznetsov, V. L., Gopal, K., Malik, M. A., Raftery, J., Edwards, P. P. & O'Brien, P. (2013). *Chem. Mater.* **25**, 266–276.
Sheldrick, G. M. (2008). *Acta Cryst.* A**64**, 112–122.
Sheldrick, G. M. (2015). *Acta Cryst.* C**71**, 3–8.
Spackman, M. A., McKinnon, J. J. & Jayatilaka, D. (2008). *CrystEngComm*, **10**, 377–388.
Spek, A. L. (2009). *Acta Cryst.* D**65**, 148–155.
Tiekink, E. R. T. (2008). *Appl. Organomet. Chem.* **22**, 533–550.
Westrip, S. P. (2010). *J. Appl. Cryst.* **43**, 920–925.
Wolff, S. K., Grimwood, D. J., McKinnon, J. J., Turner, M. J., Jayatilaka, D. & Spackman, M. A. (2012). *Crystal Explorer*. The University of Western Australia.
Yu, Y., Yang, H., Wei, Z.-W. & Tang, L.-F. (2014). *Heteroat. Chem.* **25**, 274–281.
Zia-ur-Rehman, Muhammad, N., Ali, S., Butler, I. S. & Meetsma, A. (2011). *Inorg. Chim. Acta*, **376**, 381–388.

supporting information

Acta Cryst. (2016). E**72**, 1130-1137 [doi:10.1107/S2056989016011385]

Distinct coordination geometries in bis[*N*,*N*-bis(2-methoxyethyl)dithiocarbamato-$\kappa^2 S,S'$]diphenyltin(IV) and bis[*N*-(2-methoxyethyl)-*N*-methyldithiocarbamato-$\kappa^2 S,S'$]diphenyltin(IV): crystal structures and Hirshfeld surface analysis

Rapidah Mohamad, Normah Awang, Mukesh M. Jotani and Edward R. T. Tiekink

Computing details

For both compounds, data collection: *CrysAlis PRO* (Agilent, 2015); cell refinement: *CrysAlis PRO* (Agilent, 2015); data reduction: *CrysAlis PRO* (Agilent, 2015); program(s) used to solve structure: *SHELXL97* (Sheldrick, 2008); program(s) used to refine structure: *SHELXL2014* (Sheldrick, 2015); molecular graphics: *ORTEP-3 for Windows* (Farrugia, 2012) and *DIAMOND* (Brandenburg, 2006). Software used to prepare material for publication: *publCIF* (Westrip, 2010) for (I); *SHELXL2014* (Sheldrick, 2015) for (II).

(I) Bis[*N*,*N*-bis(2-methoxyethyl)dithiocarbamato-$\kappa^2 S,S'$]diphenyltin(IV)

Crystal data

$[Sn(C_6H_5)_2(C_5H_{10}NOS_2)_2]$
M_r = 601.41
Monoclinic, *C*2/*c*
a = 18.3808 (14) Å
b = 8.2809 (4) Å
c = 19.083 (3) Å
β = 118.071 (8)°
V = 2562.9 (5) Å^3
Z = 4
F(000) = 1224
D_x = 1.559 Mg m^{-3}
Mo *K*α radiation, λ = 0.71073 Å
Cell parameters from 3633 reflections
θ = 4.2–29.9°
μ = 1.34 mm^{-1}
T = 293 K
Block, colourless
0.25 × 0.25 × 0.20 mm

Data collection

Agilent Technologies SuperNova Dual diffractometer with Atlas detector
Radiation source: SuperNova (Mo) X-ray Source
Mirror monochromator
Detector resolution: 10.4041 pixels mm^{-1}
ω scan
Absorption correction: multi-scan (CrysAlis PRO; Agilent, 2015)
T_{min} = 0.815, T_{max} = 1.000
7357 measured reflections
3383 independent reflections
3051 reflections with $I > 2\sigma(I)$
R_{int} = 0.025
θ_{max} = 30.4°, θ_{min} = 4.0°
h = −26→18
k = −11→11
l = −25→26

Refinement

Refinement on F^2
Least-squares matrix: full
$R[F^2 > 2\sigma(F^2)]$ = 0.026
$wR(F^2)$ = 0.063
S = 1.07
3383 reflections
143 parameters
0 restraints

Hydrogen site location: inferred from neighbouring sites
H-atom parameters constrained

$w = 1/[\sigma^2(F_o^2) + (0.0284P)^2 + 0.8262P]$ where $P = (F_o^2 + 2F_c^2)/3$
$(\Delta/\sigma)_{max} = 0.001$
$\Delta\rho_{max} = 0.47$ e Å^{-3}
$\Delta\rho_{min} = -0.30$ e Å^{-3}

Special details

Geometry. All esds (except the esd in the dihedral angle between two l.s. planes) are estimated using the full covariance matrix. The cell esds are taken into account individually in the estimation of esds in distances, angles and torsion angles; correlations between esds in cell parameters are only used when they are defined by crystal symmetry. An approximate (isotropic) treatment of cell esds is used for estimating esds involving l.s. planes.

Fractional atomic coordinates and isotropic or equivalent isotropic displacement parameters (Å²)

	x	*y*	*z*	U_{iso}*/U_{eq}
Sn	0.5000	0.56549 (2)	0.7500	0.03252 (7)
S1	0.65567 (3)	0.64166 (6)	0.82876 (3)	0.04210 (12)
S2	0.52661 (3)	0.81055 (7)	0.84973 (4)	0.04728 (13)
O1	0.77790 (11)	1.16594 (19)	0.88988 (10)	0.0563 (4)
N1	0.68188 (11)	0.90857 (19)	0.91561 (10)	0.0391 (4)
C1	0.62737 (11)	0.8001 (2)	0.87001 (11)	0.0350 (4)
C2	0.65719 (17)	1.0454 (3)	0.94849 (16)	0.0568 (6)
H2A	0.6227	1.1170	0.9063	0.068*
H2B	0.7054	1.1024	0.9858	0.068*
H2C	0.6273	1.0063	0.9749	0.068*
C3	0.76876 (13)	0.9020 (3)	0.93400 (13)	0.0458 (5)
H3A	0.7836	0.7905	0.9316	0.055*
H3B	0.8025	0.9398	0.9879	0.055*
C4	0.78779 (13)	1.0011 (3)	0.87883 (13)	0.0464 (5)
H4A	0.8440	0.9808	0.8893	0.056*
H4B	0.7511	0.9709	0.8243	0.056*
C5	0.80091 (16)	1.2685 (3)	0.84467 (16)	0.0630 (7)
H5A	0.8589	1.2570	0.8620	0.095*
H5B	0.7890	1.3784	0.8516	0.095*
H5C	0.7705	1.2398	0.7896	0.095*
C11	0.52133 (11)	0.3974 (2)	0.67451 (11)	0.0337 (4)
C12	0.57526 (14)	0.2710 (3)	0.71091 (13)	0.0470 (5)
H12	0.6002	0.2605	0.7659	0.056*
C13	0.59275 (15)	0.1597 (3)	0.66667 (15)	0.0552 (6)
H13	0.6294	0.0758	0.6920	0.066*
C14	0.55615 (14)	0.1732 (3)	0.58582 (15)	0.0525 (6)
H14	0.5679	0.0986	0.5561	0.063*
C15	0.50225 (14)	0.2964 (3)	0.54873 (13)	0.0512 (5)
H15	0.4771	0.3052	0.4937	0.061*
C16	0.48494 (13)	0.4085 (3)	0.59275 (12)	0.0425 (4)
H16	0.4483	0.4923	0.5669	0.051*

Atomic displacement parameters (Å²)

	U^{11}	U^{22}	U^{33}	U^{12}	U^{13}	U^{23}
Sn	0.03241 (10)	0.03268 (10)	0.03421 (10)	0.000	0.01712 (7)	0.000
S1	0.0349 (2)	0.0430 (3)	0.0492 (3)	0.0002 (2)	0.0205 (2)	−0.0098 (2)
S2	0.0413 (3)	0.0423 (3)	0.0667 (4)	−0.0031 (2)	0.0324 (3)	−0.0114 (2)
O1	0.0732 (11)	0.0438 (8)	0.0706 (11)	−0.0030 (8)	0.0492 (9)	0.0028 (7)
N1	0.0423 (9)	0.0359 (8)	0.0404 (9)	−0.0064 (7)	0.0205 (7)	−0.0038 (7)
C1	0.0380 (9)	0.0340 (9)	0.0363 (9)	−0.0004 (8)	0.0202 (8)	0.0018 (7)
C2	0.0753 (17)	0.0458 (12)	0.0653 (15)	−0.0149 (12)	0.0464 (14)	−0.0188 (11)
C3	0.0362 (10)	0.0428 (11)	0.0470 (12)	−0.0037 (9)	0.0102 (8)	0.0021 (9)
C4	0.0399 (10)	0.0475 (11)	0.0539 (12)	−0.0014 (10)	0.0238 (9)	−0.0044 (10)
C5	0.0649 (16)	0.0613 (15)	0.0704 (17)	−0.0060 (13)	0.0381 (13)	0.0137 (13)
C11	0.0331 (9)	0.0349 (9)	0.0345 (9)	−0.0020 (8)	0.0171 (7)	−0.0019 (7)
C12	0.0529 (12)	0.0457 (11)	0.0374 (10)	0.0098 (10)	0.0169 (9)	0.0000 (9)
C13	0.0552 (13)	0.0432 (12)	0.0634 (15)	0.0122 (11)	0.0248 (11)	−0.0053 (10)
C14	0.0552 (13)	0.0515 (13)	0.0627 (14)	−0.0112 (11)	0.0377 (11)	−0.0230 (11)
C15	0.0549 (13)	0.0636 (14)	0.0371 (11)	−0.0127 (12)	0.0234 (9)	−0.0111 (10)
C16	0.0391 (10)	0.0483 (11)	0.0371 (10)	0.0014 (9)	0.0153 (8)	0.0016 (8)

Geometric parameters (Å, º)

Sn—C11	2.1677 (18)	C3—H3B	0.9700
Sn—C11^{i}	2.1678 (18)	C4—H4A	0.9700
Sn—S1	2.6071 (6)	C4—H4B	0.9700
Sn—S1^{i}	2.6071 (6)	C5—H5A	0.9600
Sn—S2^{i}	2.6653 (6)	C5—H5B	0.9600
Sn—S2	2.6653 (6)	C5—H5C	0.9600
S1—C1	1.7311 (19)	C11—C16	1.381 (3)
S2—C1	1.7067 (19)	C11—C12	1.383 (3)
O1—C4	1.406 (3)	C12—C13	1.386 (3)
O1—C5	1.410 (3)	C12—H12	0.9300
N1—C1	1.322 (2)	C13—C14	1.367 (3)
N1—C3	1.466 (3)	C13—H13	0.9300
N1—C2	1.467 (3)	C14—C15	1.365 (3)
C2—H2A	0.9600	C14—H14	0.9300
C2—H2B	0.9600	C15—C16	1.386 (3)
C2—H2C	0.9600	C15—H15	0.9300
C3—C4	1.500 (3)	C16—H16	0.9300
C3—H3A	0.9700		
C11—Sn—C11^{i}	100.07 (10)	N1—C3—H3B	108.9
C11—Sn—S1	92.63 (5)	C4—C3—H3B	108.9
C11^{i}—Sn—S1	105.36 (5)	H3A—C3—H3B	107.7
C11—Sn—S1^{i}	105.36 (5)	O1—C4—C3	109.68 (18)
C11^{i}—Sn—S1^{i}	92.63 (5)	O1—C4—H4A	109.7
S1—Sn—S1^{i}	152.00 (2)	C3—C4—H4A	109.7
C11—Sn—S2^{i}	92.54 (5)	O1—C4—H4B	109.7

C11^{i}—Sn—S2^{i}	159.03 (5)	C3—C4—H4B	109.7
S1—Sn—S2^{i}	90.591 (19)	H4A—C4—H4B	108.2
S1^{i}—Sn—S2^{i}	67.742 (17)	O1—C5—H5A	109.5
C11—Sn—S2	159.03 (5)	O1—C5—H5B	109.5
C11^{i}—Sn—S2	92.54 (5)	H5A—C5—H5B	109.5
S1—Sn—S2	67.744 (17)	O1—C5—H5C	109.5
S1^{i}—Sn—S2	90.590 (19)	H5A—C5—H5C	109.5
S2^{i}—Sn—S2	80.82 (3)	H5B—C5—H5C	109.5
C1—S1—Sn	87.84 (6)	C16—C11—C12	118.01 (18)
C1—S2—Sn	86.46 (7)	C16—C11—Sn	124.38 (14)
C4—O1—C5	113.31 (18)	C12—C11—Sn	117.61 (14)
C1—N1—C3	122.35 (17)	C11—C12—C13	120.9 (2)
C1—N1—C2	121.01 (18)	C11—C12—H12	119.5
C3—N1—C2	116.62 (18)	C13—C12—H12	119.5
N1—C1—S2	121.35 (15)	C14—C13—C12	120.1 (2)
N1—C1—S1	121.16 (14)	C14—C13—H13	120.0
S2—C1—S1	117.49 (11)	C12—C13—H13	120.0
N1—C2—H2A	109.5	C15—C14—C13	119.87 (19)
N1—C2—H2B	109.5	C15—C14—H14	120.1
H2A—C2—H2B	109.5	C13—C14—H14	120.1
N1—C2—H2C	109.5	C14—C15—C16	120.3 (2)
H2A—C2—H2C	109.5	C14—C15—H15	119.9
H2B—C2—H2C	109.5	C16—C15—H15	119.9
N1—C3—C4	113.51 (17)	C11—C16—C15	120.8 (2)
N1—C3—H3A	108.9	C11—C16—H16	119.6
C4—C3—H3A	108.9	C15—C16—H16	119.6
C3—N1—C1—S2	179.88 (15)	C5—O1—C4—C3	175.27 (19)
C2—N1—C1—S2	−2.0 (3)	N1—C3—C4—O1	67.0 (2)
C3—N1—C1—S1	0.0 (3)	C16—C11—C12—C13	0.5 (3)
C2—N1—C1—S1	178.13 (16)	Sn—C11—C12—C13	−179.24 (17)
Sn—S2—C1—N1	173.67 (16)	C11—C12—C13—C14	−0.4 (4)
Sn—S2—C1—S1	−6.47 (10)	C12—C13—C14—C15	−0.1 (3)
Sn—S1—C1—N1	−173.53 (16)	C13—C14—C15—C16	0.4 (3)
Sn—S1—C1—S2	6.60 (10)	C12—C11—C16—C15	−0.2 (3)
C1—N1—C3—C4	93.8 (2)	Sn—C11—C16—C15	179.59 (16)
C2—N1—C3—C4	−84.4 (2)	C14—C15—C16—C11	−0.3 (3)

Symmetry code: (i) −*x*+1, *y*, −*z*+3/2.

Hydrogen-bond geometry (Å, º)

Cg1 is the centroid of the C11–C16 phenyl ring.

D—H···*A*	*D*—H	H···*A*	*D*···*A*	*D*—H···*A*
C4—H4*A*···*Cg*1^{ii}	0.97	2.86	3.730 (3)	150

Symmetry code: (ii) *x*+1, −*y*, *z*+1/2.

(II) Bis[*N*-(2-methoxyethyl)-*N*-methyldithiocarbamato-κ^2S,S']diphenyltin(IV)

Crystal data

$[Sn(C_6H_5)_2(C_7H_{14}NO_2S_2)_2]$
$M_r = 689.51$
Triclinic, $P\overline{1}$
$a = 7.4386$ (4) Å
$b = 14.3334$ (8) Å
$c = 16.5398$ (10) Å
$\alpha = 110.320$ (5)°
$\beta = 91.282$ (5)°
$\gamma = 101.865$ (4)°
$V = 1609.93$ (17) Å^3
$Z = 2$
$F(000) = 708$
$D_x = 1.422$ Mg m^{-3}
Mo $K\alpha$ radiation, $\lambda = 0.71073$ Å
Cell parameters from 6877 reflections
$\theta = 3.8$–$29.7°$
$\mu = 1.09$ mm^{-1}
$T = 293$ K
Block, colourless
0.30 × 0.25 × 0.25 mm

Data collection

Agilent Technologies SuperNova Dual diffractometer with Atlas detector
Radiation source: SuperNova (Mo) X-ray Source
Mirror monochromator
Detector resolution: 10.4041 pixels mm^{-1}
ω scan
Absorption correction: multi-scan (CrysAlis PRO; Agilent, 2015)
$T_{min} = 0.756$, $T_{max} = 1.000$
17063 measured reflections
8354 independent reflections
6973 reflections with $I > 2\sigma(I)$
$R_{int} = 0.035$
$\theta_{max} = 30.4°$, $\theta_{min} = 3.3°$
$h = -10 \rightarrow 10$
$k = -19 \rightarrow 19$
$l = -22 \rightarrow 18$

Refinement

Refinement on F^2
Least-squares matrix: full
$R[F^2 > 2\sigma(F^2)] = 0.031$
$wR(F^2) = 0.078$
$S = 1.06$
8354 reflections
338 parameters
0 restraints
Hydrogen site location: inferred from neighbouring sites
H-atom parameters constrained
$w = 1/[\sigma^2(F_o^2) + (0.0316P)^2 + 0.0774P]$ where $P = (F_o^2 + 2F_c^2)/3$
$(\Delta/\sigma)_{max} = 0.002$
$\Delta\rho_{max} = 0.66$ e Å^{-3}
$\Delta\rho_{min} = -0.56$ e Å^{-3}

Special details

Geometry. All esds (except the esd in the dihedral angle between two l.s. planes) are estimated using the full covariance matrix. The cell esds are taken into account individually in the estimation of esds in distances, angles and torsion angles; correlations between esds in cell parameters are only used when they are defined by crystal symmetry. An approximate (isotropic) treatment of cell esds is used for estimating esds involving l.s. planes.

Fractional atomic coordinates and isotropic or equivalent isotropic displacement parameters (Å^2)

	x	*y*	*z*	U_{iso}*/U_{eq}
Sn	0.53321 (2)	0.25616 (2)	0.25381 (2)	0.04036 (6)
S1	0.34463 (8)	0.37273 (4)	0.23099 (4)	0.05095 (14)
S2	0.75066 (8)	0.44734 (5)	0.23709 (5)	0.05550 (15)
S3	0.22105 (8)	0.15139 (4)	0.26109 (4)	0.04817 (14)
S4	0.53671 (8)	0.06041 (4)	0.27883 (4)	0.04702 (13)
O1	0.3430 (3)	0.61622 (18)	0.10117 (16)	0.1049 (8)
O2	0.6103 (3)	0.75288 (15)	0.38247 (15)	0.0899 (7)
O3	−0.0963 (3)	−0.19679 (12)	0.15238 (12)	0.0705 (5)
O4	0.1455 (3)	−0.09606 (15)	0.42343 (13)	0.0737 (5)

N1	0.5046 (3)	0.55831 (13)	0.23494 (13)	0.0504 (4)
N2	0.1846 (2)	−0.03099 (12)	0.27492 (12)	0.0426 (4)
C1	0.5361 (3)	0.46932 (15)	0.23417 (14)	0.0437 (5)
C2	0.3173 (4)	0.57560 (18)	0.22800 (18)	0.0601 (6)
H2A	0.3202	0.6469	0.2604	0.072*
H2B	0.2358	0.5348	0.2542	0.072*
C3	0.2400 (4)	0.5493 (2)	0.1363 (2)	0.0750 (8)
H3A	0.2446	0.4796	0.1022	0.090*
H3B	0.1121	0.5544	0.1349	0.090*
C4	0.2821 (6)	0.5939 (3)	0.0126 (3)	0.1359 (18)
H4A	0.2869	0.5249	−0.0211	0.204*
H4B	0.3609	0.6400	−0.0090	0.204*
H4C	0.1575	0.6016	0.0082	0.204*
C5	0.6601 (4)	0.64484 (18)	0.24329 (19)	0.0653 (7)
H5A	0.6178	0.6911	0.2202	0.078*
H5B	0.7560	0.6194	0.2093	0.078*
C6	0.7398 (4)	0.70258 (18)	0.3363 (2)	0.0707 (8)
H6A	0.7695	0.6555	0.3620	0.085*
H6B	0.8526	0.7520	0.3387	0.085*
C7	0.6699 (6)	0.8058 (3)	0.4717 (3)	0.1109 (13)
H7A	0.7157	0.7615	0.4951	0.166*
H7B	0.5680	0.8271	0.5018	0.166*
H7C	0.7665	0.8647	0.4787	0.166*
C8	0.3058 (3)	0.05076 (14)	0.27243 (13)	0.0379 (4)
C9	−0.0177 (3)	−0.03932 (16)	0.27130 (16)	0.0485 (5)
H9A	−0.0407	0.0288	0.2931	0.058*
H9B	−0.0687	−0.0744	0.3092	0.058*
C10	−0.1160 (3)	−0.09513 (17)	0.18215 (17)	0.0562 (6)
H10A	−0.2459	−0.0940	0.1833	0.067*
H10B	−0.0646	−0.0617	0.1432	0.067*
C11	−0.1881 (5)	−0.2554 (2)	0.0696 (2)	0.0932 (10)
H11A	−0.3185	−0.2603	0.0715	0.140*
H11B	−0.1642	−0.3226	0.0516	0.140*
H11C	−0.1445	−0.2235	0.0293	0.140*
C12	0.2468 (3)	−0.11869 (16)	0.28315 (16)	0.0517 (6)
H12A	0.3521	−0.1291	0.2503	0.062*
H12B	0.1485	−0.1796	0.2581	0.062*
C13	0.3001 (4)	−0.10467 (19)	0.37586 (18)	0.0602 (6)
H13A	0.3463	−0.1626	0.3775	0.072*
H13B	0.3977	−0.0436	0.4017	0.072*
C14	0.1853 (5)	−0.0891 (3)	0.5099 (2)	0.0997 (11)
H14A	0.2197	−0.1503	0.5095	0.150*
H14B	0.0779	−0.0812	0.5404	0.150*
H14C	0.2852	−0.0313	0.5383	0.150*
C21	0.6777 (3)	0.32313 (15)	0.38043 (14)	0.0465 (5)
C22	0.5984 (5)	0.3759 (3)	0.4491 (2)	0.0928 (11)
H22	0.4791	0.3839	0.4411	0.111*
C23	0.6951 (7)	0.4189 (3)	0.5326 (2)	0.1190 (14)

H23	0.6389	0.4546	0.5795	0.143*
C24	0.8694 (6)	0.4084 (3)	0.5450 (2)	0.0970 (11)
H24	0.9330	0.4362	0.6001	0.116*
C25	0.9485 (5)	0.3575 (3)	0.4769 (2)	0.0938 (10)
H25	1.0692	0.3514	0.4846	0.113*
C26	0.8533 (4)	0.3138 (2)	0.3950 (2)	0.0783 (8)
H26	0.9102	0.2773	0.3489	0.094*
C31	0.6273 (3)	0.18363 (15)	0.13244 (14)	0.0434 (5)
C32	0.7940 (4)	0.1564 (2)	0.12717 (18)	0.0705 (7)
H32	0.8682	0.1699	0.1777	0.085*
C33	0.8533 (5)	0.1092 (2)	0.0478 (2)	0.0849 (9)
H33	0.9680	0.0926	0.0452	0.102*
C34	0.7435 (5)	0.0869 (2)	−0.0269 (2)	0.0854 (10)
H34	0.7827	0.0541	−0.0802	0.102*
C35	0.5772 (5)	0.1128 (3)	−0.02322 (19)	0.0885 (9)
H35	0.5030	0.0979	−0.0741	0.106*
C36	0.5176 (4)	0.1613 (2)	0.05655 (17)	0.0679 (7)
H36	0.4037	0.1788	0.0588	0.081*

Atomic displacement parameters (Å²)

	U^{11}	U^{22}	U^{33}	U^{12}	U^{13}	U^{23}
Sn	0.04240 (9)	0.04311 (9)	0.03293 (9)	0.01125 (6)	0.00010 (6)	0.00979 (6)
S1	0.0453 (3)	0.0431 (3)	0.0648 (4)	0.0074 (2)	−0.0022 (3)	0.0219 (3)
S2	0.0474 (3)	0.0555 (3)	0.0646 (4)	0.0082 (3)	0.0016 (3)	0.0251 (3)
S3	0.0418 (3)	0.0453 (3)	0.0620 (4)	0.0144 (2)	0.0033 (3)	0.0225 (3)
S4	0.0401 (3)	0.0506 (3)	0.0527 (3)	0.0140 (2)	0.0016 (2)	0.0195 (3)
O1	0.1032 (17)	0.1125 (17)	0.1005 (19)	−0.0200 (14)	−0.0375 (14)	0.0683 (15)
O2	0.0898 (15)	0.0732 (12)	0.0901 (16)	0.0321 (12)	−0.0235 (13)	0.0031 (11)
O3	0.0802 (13)	0.0559 (9)	0.0617 (12)	0.0067 (9)	−0.0153 (10)	0.0105 (8)
O4	0.0601 (11)	0.1001 (13)	0.0594 (12)	0.0032 (10)	−0.0044 (9)	0.0357 (11)
N1	0.0556 (11)	0.0430 (9)	0.0524 (12)	0.0066 (9)	−0.0052 (9)	0.0202 (8)
N2	0.0421 (9)	0.0402 (8)	0.0448 (11)	0.0111 (8)	0.0011 (8)	0.0136 (7)
C1	0.0486 (12)	0.0456 (11)	0.0344 (11)	0.0073 (10)	−0.0027 (9)	0.0136 (9)
C2	0.0646 (16)	0.0489 (12)	0.0689 (18)	0.0157 (12)	−0.0036 (13)	0.0227 (12)
C3	0.0669 (17)	0.0748 (17)	0.086 (2)	0.0054 (15)	−0.0199 (16)	0.0403 (16)
C4	0.133 (4)	0.164 (4)	0.107 (3)	−0.033 (3)	−0.053 (3)	0.087 (3)
C5	0.0717 (17)	0.0493 (13)	0.077 (2)	0.0013 (12)	−0.0020 (15)	0.0326 (13)
C6	0.0644 (16)	0.0480 (13)	0.090 (2)	−0.0012 (13)	−0.0163 (16)	0.0221 (13)
C7	0.108 (3)	0.094 (2)	0.100 (3)	0.030 (2)	−0.032 (2)	−0.003 (2)
C8	0.0403 (10)	0.0401 (10)	0.0314 (10)	0.0118 (9)	0.0005 (8)	0.0090 (8)
C9	0.0394 (11)	0.0484 (11)	0.0567 (15)	0.0088 (10)	0.0086 (10)	0.0182 (10)
C10	0.0425 (12)	0.0621 (14)	0.0610 (16)	0.0094 (11)	−0.0017 (11)	0.0205 (12)
C11	0.112 (3)	0.0767 (19)	0.065 (2)	−0.0041 (19)	−0.0185 (19)	0.0101 (15)
C12	0.0549 (13)	0.0387 (11)	0.0620 (16)	0.0134 (10)	0.0037 (12)	0.0172 (10)
C13	0.0572 (15)	0.0578 (13)	0.0698 (18)	0.0119 (12)	−0.0072 (13)	0.0296 (13)
C14	0.091 (2)	0.139 (3)	0.065 (2)	−0.006 (2)	−0.0112 (18)	0.051 (2)
C21	0.0552 (13)	0.0422 (10)	0.0364 (12)	0.0048 (10)	−0.0065 (10)	0.0113 (9)

C22	0.078 (2)	0.129 (3)	0.0483 (18)	0.027 (2)	−0.0008 (16)	0.0015 (18)
C23	0.134 (4)	0.152 (4)	0.0401 (19)	0.031 (3)	0.005 (2)	−0.002 (2)
C24	0.120 (3)	0.095 (2)	0.053 (2)	−0.011 (2)	−0.034 (2)	0.0211 (17)
C25	0.085 (2)	0.103 (2)	0.083 (3)	0.008 (2)	−0.038 (2)	0.032 (2)
C26	0.0730 (18)	0.093 (2)	0.0608 (19)	0.0302 (17)	−0.0145 (15)	0.0118 (15)
C31	0.0480 (12)	0.0468 (11)	0.0353 (11)	0.0125 (10)	0.0057 (9)	0.0135 (9)
C32	0.0602 (16)	0.102 (2)	0.0458 (16)	0.0309 (16)	0.0052 (13)	0.0150 (14)
C33	0.0707 (19)	0.113 (2)	0.070 (2)	0.0390 (19)	0.0278 (18)	0.0204 (18)
C34	0.099 (2)	0.102 (2)	0.0453 (18)	0.026 (2)	0.0291 (18)	0.0118 (16)
C35	0.097 (2)	0.124 (3)	0.0359 (16)	0.029 (2)	0.0013 (16)	0.0161 (16)
C36	0.0669 (16)	0.0914 (19)	0.0438 (15)	0.0282 (15)	−0.0009 (13)	0.0169 (13)

Geometric parameters (Å, º)

Sn—C31	2.124 (2)	C7—H7C	0.9600
Sn—C21	2.131 (2)	C9—C10	1.497 (3)
Sn—S1	2.5060 (6)	C9—H9A	0.9700
Sn—S3	2.5230 (6)	C9—H9B	0.9700
Sn—S4	2.9800 (6)	C10—H10A	0.9700
Sn—S2	2.9875 (6)	C10—H10B	0.9700
S1—C1	1.756 (2)	C11—H11A	0.9600
S2—C1	1.692 (2)	C11—H11B	0.9600
S3—C8	1.752 (2)	C11—H11C	0.9600
S4—C8	1.692 (2)	C12—C13	1.508 (4)
O1—C3	1.396 (3)	C12—H12A	0.9700
O1—C4	1.428 (4)	C12—H12B	0.9700
O2—C6	1.403 (3)	C13—H13A	0.9700
O2—C7	1.416 (4)	C13—H13B	0.9700
O3—C11	1.403 (3)	C14—H14A	0.9600
O3—C10	1.407 (3)	C14—H14B	0.9600
O4—C13	1.410 (3)	C14—H14C	0.9600
O4—C14	1.419 (3)	C21—C22	1.351 (4)
N1—C1	1.339 (3)	C21—C26	1.364 (4)
N1—C2	1.474 (3)	C22—C23	1.410 (5)
N1—C5	1.476 (3)	C22—H22	0.9300
N2—C8	1.337 (2)	C23—C24	1.355 (5)
N2—C12	1.472 (3)	C23—H23	0.9300
N2—C9	1.483 (3)	C24—C25	1.335 (5)
C2—C3	1.499 (4)	C24—H24	0.9300
C2—H2A	0.9700	C25—C26	1.383 (4)
C2—H2B	0.9700	C25—H25	0.9300
C3—H3A	0.9700	C26—H26	0.9300
C3—H3B	0.9700	C31—C32	1.370 (3)
C4—H4A	0.9600	C31—C36	1.383 (3)
C4—H4B	0.9600	C32—C33	1.381 (4)
C4—H4C	0.9600	C32—H32	0.9300
C5—C6	1.509 (4)	C33—C34	1.367 (5)
C5—H5A	0.9700	C33—H33	0.9300

C5—H5B	0.9700	C34—C35	1.359 (5)
C6—H6A	0.9700	C34—H34	0.9300
C6—H6B	0.9700	C35—C36	1.392 (4)
C7—H7A	0.9600	C35—H35	0.9300
C7—H7B	0.9600	C36—H36	0.9300
C31—Sn—C21	130.12 (9)	N2—C9—H9A	108.8
C31—Sn—S1	106.70 (6)	C10—C9—H9A	108.8
C21—Sn—S1	109.72 (6)	N2—C9—H9B	108.8
C31—Sn—S3	108.44 (6)	C10—C9—H9B	108.8
C21—Sn—S3	108.85 (6)	H9A—C9—H9B	107.7
S1—Sn—S3	82.873 (18)	O3—C10—C9	109.5 (2)
C31—Sn—S4	83.63 (5)	O3—C10—H10A	109.8
C21—Sn—S4	83.60 (6)	C9—C10—H10A	109.8
S1—Sn—S4	147.433 (18)	O3—C10—H10B	109.8
S3—Sn—S4	64.591 (16)	C9—C10—H10B	109.8
C31—Sn—S2	83.87 (5)	H10A—C10—H10B	108.2
C21—Sn—S2	81.92 (6)	O3—C11—H11A	109.5
S1—Sn—S2	64.922 (18)	O3—C11—H11B	109.5
S3—Sn—S2	147.742 (18)	H11A—C11—H11B	109.5
S4—Sn—S2	147.642 (17)	O3—C11—H11C	109.5
C1—S1—Sn	94.83 (7)	H11A—C11—H11C	109.5
C1—S2—Sn	80.40 (7)	H11B—C11—H11C	109.5
C8—S3—Sn	95.15 (7)	N2—C12—C13	112.95 (19)
C8—S4—Sn	81.36 (7)	N2—C12—H12A	109.0
C3—O1—C4	113.0 (3)	C13—C12—H12A	109.0
C6—O2—C7	113.3 (2)	N2—C12—H12B	109.0
C11—O3—C10	113.3 (2)	C13—C12—H12B	109.0
C13—O4—C14	112.2 (2)	H12A—C12—H12B	107.8
C1—N1—C2	122.75 (19)	O4—C13—C12	109.9 (2)
C1—N1—C5	120.5 (2)	O4—C13—H13A	109.7
C2—N1—C5	116.75 (18)	C12—C13—H13A	109.7
C8—N2—C12	121.08 (17)	O4—C13—H13B	109.7
C8—N2—C9	123.23 (17)	C12—C13—H13B	109.7
C12—N2—C9	115.69 (17)	H13A—C13—H13B	108.2
N1—C1—S2	122.83 (17)	O4—C14—H14A	109.5
N1—C1—S1	117.81 (17)	O4—C14—H14B	109.5
S2—C1—S1	119.36 (12)	H14A—C14—H14B	109.5
N1—C2—C3	113.2 (2)	O4—C14—H14C	109.5
N1—C2—H2A	108.9	H14A—C14—H14C	109.5
C3—C2—H2A	108.9	H14B—C14—H14C	109.5
N1—C2—H2B	108.9	C22—C21—C26	117.7 (3)
C3—C2—H2B	108.9	C22—C21—Sn	121.2 (2)
H2A—C2—H2B	107.8	C26—C21—Sn	121.12 (19)
O1—C3—C2	109.5 (2)	C21—C22—C23	120.5 (3)
O1—C3—H3A	109.8	C21—C22—H22	119.7
C2—C3—H3A	109.8	C23—C22—H22	119.7
O1—C3—H3B	109.8	C24—C23—C22	120.3 (3)

C2—C3—H3B	109.8	C24—C23—H23	119.8
H3A—C3—H3B	108.2	C22—C23—H23	119.8
O1—C4—H4A	109.5	C25—C24—C23	119.1 (3)
O1—C4—H4B	109.5	C25—C24—H24	120.5
H4A—C4—H4B	109.5	C23—C24—H24	120.5
O1—C4—H4C	109.5	C24—C25—C26	120.8 (3)
H4A—C4—H4C	109.5	C24—C25—H25	119.6
H4B—C4—H4C	109.5	C26—C25—H25	119.6
N1—C5—C6	112.0 (2)	C21—C26—C25	121.5 (3)
N1—C5—H5A	109.2	C21—C26—H26	119.2
C6—C5—H5A	109.2	C25—C26—H26	119.2
N1—C5—H5B	109.2	C32—C31—C36	118.6 (2)
C6—C5—H5B	109.2	C32—C31—Sn	121.56 (18)
H5A—C5—H5B	107.9	C36—C31—Sn	119.81 (17)
O2—C6—C5	109.2 (2)	C31—C32—C33	120.9 (3)
O2—C6—H6A	109.8	C31—C32—H32	119.5
C5—C6—H6A	109.8	C33—C32—H32	119.5
O2—C6—H6B	109.8	C34—C33—C32	120.0 (3)
C5—C6—H6B	109.8	C34—C33—H33	120.0
H6A—C6—H6B	108.3	C32—C33—H33	120.0
O2—C7—H7A	109.5	C35—C34—C33	120.1 (3)
O2—C7—H7B	109.5	C35—C34—H34	120.0
H7A—C7—H7B	109.5	C33—C34—H34	120.0
O2—C7—H7C	109.5	C34—C35—C36	120.1 (3)
H7A—C7—H7C	109.5	C34—C35—H35	119.9
H7B—C7—H7C	109.5	C36—C35—H35	119.9
N2—C8—S4	122.77 (15)	C31—C36—C35	120.2 (3)
N2—C8—S3	118.40 (15)	C31—C36—H36	119.9
S4—C8—S3	118.83 (11)	C35—C36—H36	119.9
N2—C9—C10	113.64 (18)		

C2—N1—C1—S2	176.85 (18)	C8—N2—C9—C10	95.7 (2)
C5—N1—C1—S2	−3.4 (3)	C12—N2—C9—C10	−85.3 (2)
C2—N1—C1—S1	−3.7 (3)	C11—O3—C10—C9	178.7 (2)
C5—N1—C1—S1	176.03 (18)	N2—C9—C10—O3	63.3 (2)
Sn—S2—C1—N1	173.13 (19)	C8—N2—C12—C13	84.5 (3)
Sn—S2—C1—S1	−6.27 (11)	C9—N2—C12—C13	−94.4 (2)
Sn—S1—C1—N1	−172.02 (16)	C14—O4—C13—C12	176.3 (2)
Sn—S1—C1—S2	7.40 (13)	N2—C12—C13—O4	62.5 (3)
C1—N1—C2—C3	−90.2 (3)	C26—C21—C22—C23	−0.4 (5)
C5—N1—C2—C3	90.0 (3)	Sn—C21—C22—C23	179.4 (3)
C4—O1—C3—C2	177.9 (3)	C21—C22—C23—C24	0.4 (6)
N1—C2—C3—O1	−66.0 (3)	C22—C23—C24—C25	0.6 (7)
C1—N1—C5—C6	−81.5 (3)	C23—C24—C25—C26	−1.6 (6)
C2—N1—C5—C6	98.3 (3)	C22—C21—C26—C25	−0.6 (5)
C7—O2—C6—C5	177.4 (2)	Sn—C21—C26—C25	179.6 (2)
N1—C5—C6—O2	−68.2 (3)	C24—C25—C26—C21	1.7 (5)
C12—N2—C8—S4	−0.3 (3)	C36—C31—C32—C33	1.1 (4)

C9—N2—C8—S4	178.62 (16)	Sn—C31—C32—C33	179.9 (2)
C12—N2—C8—S3	179.16 (16)	C31—C32—C33—C34	−1.5 (5)
C9—N2—C8—S3	−2.0 (3)	C32—C33—C34—C35	1.1 (5)
Sn—S4—C8—N2	177.09 (18)	C33—C34—C35—C36	−0.4 (5)
Sn—S4—C8—S3	−2.32 (11)	C32—C31—C36—C35	−0.4 (4)
Sn—S3—C8—N2	−176.72 (15)	Sn—C31—C36—C35	−179.3 (2)
Sn—S3—C8—S4	2.72 (13)	C34—C35—C36—C31	0.1 (5)

Hydrogen-bond geometry (Å, º)

D—H···*A*	*D*—H	H···*A*	*D*···*A*	*D*—H···*A*
C13—H13*A*···O2^{i}	0.97	2.52	3.404 (4)	151

Symmetry code: (i) *x*, *y*−1, *z*.